

# BENDING OF TIP-LOADED CFRP STIFFENED PULTRUDED GRP CANTILEVERS: COMPARISON BETWEEN THEORY AND EXPERIMENT

Geoffrey J. Turvey

*Engineering Dept., Lancaster University, Lancaster, England*

## ABSTRACT

New equations are derived for predicting the serviceability (deformation) response of partially CFRP stiffened pultruded GRP cantilevers. The analogy between the deformation response of a simply supported beam in three-point flexure and a tip-loaded cantilever allows deformation data, obtained from a series of three-point flexure tests, to be used to verify the deformations predicted with the equations. It is shown that the maximum differences between the predicted tip deflections and rotations and those measured in the tests are less than 6% and 8% respectively. Therefore, it is concluded that the new equations may be used to assess the serviceability (deformation) limit state of tip-loaded partially CFRP stiffened pultruded GRP cantilevers.

## 1. INTRODUCTION

Compared to steel or aluminium sections, pultruded GRP sections have a number of advantageous properties such as lower self-weight, higher corrosion resistance, higher electrical resistance, lower thermal conductivity etc. However, from a structural design standpoint, these advantageous characteristics are compromised by the relatively low modulus and, hence, lower flexural stiffness of GRP. The latter is the principal reason why pultruded GRP sections are used mainly in *secondary* load bearing structures. Even so, there is a growing number of instances of their use in *primary* load bearing structures such as access bridges and buildings. Noteworthy examples in Europe are: the Kolding Bridge in Denmark, the Bond's Mill lift bridge in the UK and the Eyecatcher Building in Switzerland. However, unless the flexural stiffness of pultruded sections vis-à-vis metallic sections can be enhanced significantly, growth of their use in primary load bearing structures is likely to remain slow.

The need to enhance the flexural stiffness of pultruded GRP sections in order to promote their wider use in infrastructure has been recognised for at least a decade and various attempts have been made to address it. There are a variety of ways in which the flexural stiffness of a pultruded GRP section may be enhanced. The simplest, and most effective, is to increase the depth of the section. Another is to replace some of the glass rovings in the extremities of the section (usually the flanges) with carbon rovings. Both approaches have been exploited successfully by the US pultrusion industry. A 610mm deep Wide Flange (WF) section with CFRP rovings in the flanges was produced in the late 1990s [1]. The depth of this section is approximately two and a half times that of the largest *off-the-shelf* structural grade WF section. Subsequently, a 914mm deep double-web beam was produced with carbon rovings in the flanges [2]. In order to make such a deep section, the world's largest pultrusion machine had to be designed, built and commissioned at a cost of several million dollars. Although these two examples have demonstrated the feasibility of manufacturing pultruded GRP profiles with flexural stiffnesses substantially larger than the largest off-the-shelf profiles, the economic case for doing so remains questionable. This is because the volume of reinforcement to be accommodated at the input end of the pultrusion line, the pulling force required at the

output end, and the overall production costs increase disproportionately with the depth of the section. Clearly, there is a maximum section depth beyond which it is uneconomic to produce integral pultruded GRP profiles. Furthermore, replacing glass rovings in the flanges with carbon rovings is limited by the cross-sectional area of the flanges. Moreover, the carbon rovings stiffen the flanges uniformly along their length which implies that the high stiffness CFRP material is not used effectively over the full length of the profile, especially near the supports of simply supported beams where the bending moments are small.

An alternative approach to achieving greater section depth is to fabricate large sections from a number of smaller pultruded sections. The Advanced Composite Construction System (ACCS) is an early, outstanding example of this approach [3]. It enables deep multi-web box beams to be fabricated from three smaller pultruded GRP components (a 600mm wide by 80mm deep multi-web flat panel, a square cross-section tube with recesses in three faces and a solid bar which acts as a toggle connection).

A more flexible, and cheaper approach (well-suited to enhancing the flexural stiffness of off-the-shelf pultruded GRP WF sections) is to bond unidirectional CFRP strip to the outer faces of the flanges. Its flexibility and efficiency derive from the fact that the thickness of the CFRP strip is not limited by the flange thickness (as is the case when glass rovings are substituted with carbon rovings) and the distribution of the strip along the beam can be tailored to the bending moment.

Recently, a number of research investigations have been carried out in order to quantify the stiffness benefits which derive from bonding CFRP strip to the flanges of pultruded GRP WF beams. In particular, the results of a series of three-point flexure tests on pultruded GRP 102 x 102 x 6.4mm WF beams of 2.95m span [4] have shown that bonding two 23.4 x 2.6mm unidirectional CFRP strips (a relatively small quantity of high modulus reinforcement) to the tension flange increased the beam's flexural stiffness by 37% (a not insignificant increase!). It is envisaged that the simple approach of bonding high modulus CFRP strip to the flanges of pultruded GRP beams may well be perceived as an effective and economical means of enhancing their flexural stiffness. In fact, structural engineers have long been familiar with this approach. They routinely use steel strip/plate to stiffen timber beams (flitched beam design) and there is growing use of CFRP strip/plate to stiffen concrete, steel and timber beams, so *designer resistance* to revitalising old technologies with new materials should not be an impediment. Moreover, design guidance for CFRP stiffened/strengthened concrete [5] and steel [6] beams is now available, which can only serve to encourage the use of modern lightweight fibre-reinforced composite materials in construction. Clearly, there is a similar need for guidance on the design of CFRP stiffened pultruded GRP beams. For some time, this deficiency has been recognised and the situation is now beginning to be addressed.

More often than not, the design of a CFRP stiffened GRP beam is governed by the deflection serviceability limit state rather than the ultimate strength limit state. Therefore, it is important to develop simple equations for predicting the deformation response of such beams. Recently, the author addressed this issue [7 & 8]. Equations were derived for the centre deflection etc of single-span CFRP stiffened GRP beams with semi-rigid end connections and subjected to uniformly distributed and mid-span point loading. Performance indices which enable the benefits, in terms of reduced deflection etc, of CFRP stiffeners to be rapidly quantified were also derived. The accuracy of the equations was verified by using them to predict deformations, measured

in three-point bending tests, of CFRP stiffened GRP beams with idealised and practical (bolted cleat) end conditions. Except for beams with clamped ends, it was shown that the equations predicted the measured deflections and rotations with errors of less than 6% and 12% respectively. The poor correlation between the predicted and measured responses for beams with clamped ends was due to the difficulty of simulating such end conditions in the tests. Thus, it remains to demonstrate conclusively that the design equations are accurate for clamped end conditions.

The design guidance reported in [7 & 8] was developed for beams supported at both ends. It is not unreasonable to expect that designers may also be required to assess the serviceability limit state of beams supported at one end only, i.e. to assess the deformation response of CFRP stiffened GRP cantilevers. Unfortunately, the equations given in [7 & 8] are not applicable to cantilever beams. Thus, the primary objectives of this paper are to derive equations for the deformation response of cantilevers and to verify their accuracy, and, by implication, to demonstrate that the equations given in [7 & 8] must also be valid for clamped end conditions.

## **2. RELATIONSHIP BETWEEN THE FLEXURAL RESPONSE OF SIMPLY SUPPORTED AND CANTILEVER BEAMS**

As explained in the Introduction, the equations, reported in [7 & 8], for CFRP stiffened pultruded beams with semi-rigid end connections did not predict the deformation response accurately when the ends were clamped. The reason for this lack of correlation was surmised to be due to the difficulty of simulating perfectly rigid supports in the beam tests. Indeed, previous research, undertaken by the author and his co-investigator, on the lateral buckling of pultruded GRP beams [9 - 11], has highlighted the difficulty of achieving truly rigid supports in tests – a variety of clamping arrangements were tried and none was entirely successful. Clearly, this experience poses difficulties for the experimental verification of the equations which will be developed for predicting the deformation response of CFRP stiffened GRP cantilevers. An alternative approach is required, preferably one which avoids clamping of the beam in attempting to suppress the rotation at the rigid support.

Fig. 1(a) shows a simply supported CFRP stiffened GRP beam subjected to a vertical point load  $Q$  at mid-span. The deflected profile of the beam is shown in Fig. 1(b). As expected, the deflected profile is symmetric about the vertical centreline and the tangent to it at mid-span is horizontal, indicating that no rotation occurs at this location as the beam deflects under the load. In this respect the centre of the beam acts like a truly rigid support. Of course, in this case (unlike that of the cantilever) the centre  $C$  of the beam deflects through  $\delta_c$  under the load  $Q$ . However, if one subtracts the deflection  $\delta_c$  from every point along the deflection profile, then the deflection at  $C$  becomes zero and the mid-span of the beam behaves as if rigidly clamped. This subtraction process implies that, relative to  $C$ , the ends  $A$  and  $B$  deflect upwards by an amount  $\delta_c$ . The rotations at  $A$ ,  $B$  and  $C$  remain unaltered by the deflection subtraction process. Thus, the simply supported beam may be envisaged as a pair of identical back-to-back cantilevers with spans half that of the simply supported beam and subjected to upward tip loads equal to half the load  $Q$  applied at mid-span. The right hand equivalent cantilever beam subjected to an upward tip load of  $Q/2$  is shown in Fig. 2(a) and its deflected profile is depicted in Fig. 2(b). The tip deformations of the cantilever,  $\delta_B$  and  $\theta_B$ , are identical with the mid-span deflection and the rotation at the right hand support of the simply supported beam [see Fig. 1(b)].

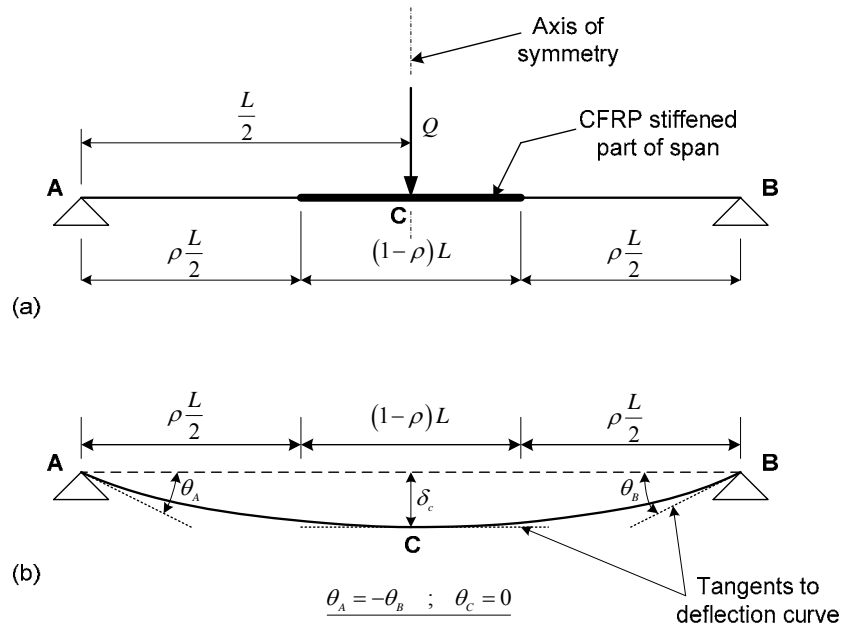


Fig. 1: A CFRP stiffened pultruded GRP beam in three-point flexure: (a) beam geometry and loading and (b) beam deformation showing mid-span deflection and end rotations.

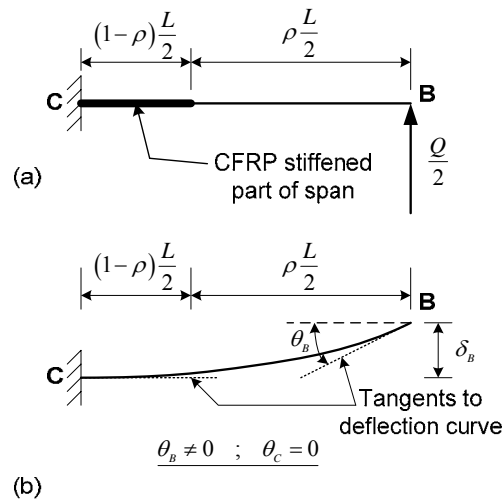


Fig. 2: A CFRP stiffened GRP cantilever: (a) beam geometry and loading and (b) beam deformation showing the tip deflection and end rotations.

From the experimental standpoint, the implications of the similarity of the relationship between the symmetrically loaded simply supported beam and the tip loaded cantilever are profound. Firstly, testing a simply supported beam instead of a cantilever beam eliminates the problems associated with simulating a single rigid support in a test. The second benefit is that deflections and rotations are measured at different positions on the beam rather than at the same position on the cantilever, thereby reducing over-crowding of the instrumentation. Moreover, the rotations may be measured at both ends of the simply supported beam and two readings will result in a more accurate average rotation

measurement. A further, fortuitous and compelling reason for preferring to use results from simply supported beam tests to verify deformation predictions from cantilever beam equations is that test results are already available in [8]. Therefore, no further testing is necessary; it only remains to derive the cantilever deformation equations and to compare the predicted results with the available test results.

### 3. DERIVATION OF DEFORMATION EQUATIONS FOR STIFFENED CANTILEVERS

In this section, equations are derived for the partially CFRP stiffened pultruded GRP cantilever depicted in Fig. 2(a). The cantilever is loaded by an upward vertical point load  $Q/2$  applied at its free end B and its other end is rigidly clamped at C. The span of the cantilever is  $L/2$ . The length of the unstiffened portion of the span is defined by the parameter  $\rho$ . Thus, when  $\rho = 1$  the cantilever is unstiffened and when  $\rho = 0$  it is stiffened along its entire span.

For the purposes of the analysis, it is assumed that  $E$  is the longitudinal elastic modulus,  $G$  is the transverse shear modulus,  $I$  is the second moment of area and  $A$  is the cross-sectional area of the pultruded GRP beam. The CFRP stiffeners (bonded to the flanges of the GRP section) are accounted for in the analysis by converting their cross-sectional area into an equivalent cross-sectional area of GRP material using the Method of Transformed Sections [12]. Therefore, the CFRP stiffened part of the cantilever is assumed to have the same longitudinal elastic and transverse shear moduli as the unstiffened part. On the other hand, the second moment of area and cross-sectional area of the CFRP stiffened part of the cantilever are  $I_s$  and  $A_s$  respectively, where  $I_s = I(1 + \phi_I)$  and  $A_s = A(1 + \phi_A)$ . In these relationships, the terms  $\phi_I$  and  $\phi_A$  denote the increase in second moment of area and cross-sectional area respectively due to the CFRP stiffening material. Formulae for their evaluation are given in [7 & 8].

Clearly, the maximum values of the deflection and rotation of the cantilever occur at its tip, as shown in Fig. 2(b). Therefore, in order to check the serviceability (deformation) limit state, formulae are required for the evaluation of  $\delta_B$  and  $\theta_B$ . Such formulae may be derived by the Method of Influence Coefficients [13]. Using this method, the general formula for the tip deflection  $\delta_B$  may be expressed as,

$$\delta_B = \int_0^{\rho \frac{L}{2}} \frac{m_0 m_\delta}{EI} dl + \int_{\rho \frac{L}{2}}^{\frac{L}{2}} \frac{m_0 m_\delta}{EI_s} dl + \int_0^{\rho \frac{L}{2}} \frac{s_0 s_\delta}{GA} dl + \int_{\rho \frac{L}{2}}^{\frac{L}{2}} \frac{s_0 s_\delta}{GA_s} dl \quad (1)$$

In Eq. 1 the first two integrals account for bending effects and the second two integrals for shear deformation effects which may be significant for fibre reinforced polymer composite materials, especially when the cantilever span is short or significant quantities of high modulus CFRP strip are bonded to the flanges of the GRP section. Normally a shear correction factor (multiplier) would be applied to  $GA$  and  $GA_s$  in the denominators of the third and fourth integrals respectively in Eq. 1. However, because the minimum value of the shear modulus  $G$  (taken from the pultruder's design handbook [14]) is used in the subsequent verification of the deformation equations it is deemed acceptable to use a unit value for the shear correction factor. Therefore, it does not appear in Eq. 1.

The terms  $m_0$  and  $m_\delta$  in Eq. 1 are the bending moment distributions due to the load  $Q/2$  and a unit vertical load respectively at the free end B of the cantilever. Likewise, the

terms  $s_0$  and  $s_\delta$  denote the shear force distributions due to the same loads. Evaluation of the four integrals on the right hand side of Eq. 1 leads to the following expression for the tip deflection of the cantilever,

$$\delta_B = \frac{QL^3}{48EI} \left[ \rho^3 + \frac{(1-\rho)(1+\rho+\rho^2)}{(1+\phi_I)} + 12\alpha \left\{ \rho + \frac{(1-\rho)}{(1+\phi_A)} \right\} \right] \quad (2)$$

An equation similar to Eq. 1 may be set up to determine the rotation at the free end of the cantilever by replacing  $\delta_B$  with  $\theta_B$  and interpreting  $m_\delta$  as the bending moment distribution due to a unit couple applied to the tip of the cantilever. The shear force distribution  $s_\delta$  is, in this case, zero. Hence, the third and fourth integrals on the right hand side of Eq. 1 do not contribute to the tip rotation, so that the equation for the tip rotation becomes,

$$\theta_B = \frac{QL^2}{16EI} \left[ \rho^2 + \frac{(1-\rho)(1+\rho)}{(1+\phi_I)} \right] \quad (3)$$

Finally, it should be appreciated that the term  $\alpha$  ( $=EI/GAL^2$ ) in Eq. 2 is a non-dimensional shear flexibility parameter.

#### 4. COMPARISON OF PREDICTED AND EXPERIMENTAL DEFORMATIONS

The analogy between the deformations of a tip loaded cantilever and those of a simply supported beam in three-point flexure is exploited to verify the accuracy of Eqs. 2 and 3. The deformation data sets given in [8] for unstiffened, CFRP partially stiffened and CFRP fully stiffened simply supported pultruded GRP beams in three-point flexure are used for this purpose. In all, four sets of data are used to compare with predicted deformations obtained from Eqs. 2 and 3.

The first set of results comparisons are for four unstiffened pultruded GRP 102 x 102 x 6.4mm WF beams, labelled A – D. The beams are nominally identical. However, tension tests were carried out on coupons cut from only one of the beams to determine their longitudinal elastic modulus. The transverse shear modulus was taken as the minimum value given in [14]. It is known that the elastic stiffnesses may vary along the length of pultruded GRP profiles and that is why the loads, given in Table 1, producing mid-span deflections of 20mm (equal to the cantilever tip deflection) in Beams A to D differ somewhat. In Eqs. 2 and 3 the values of E and G were taken as 21.11kN/mm<sup>2</sup> and 2.93kN/mm<sup>2</sup> respectively. Moreover, the span L (of the simply supported beams) was 2.5m and because the GRP beams were unstiffened  $\phi_I$  and  $\phi_A$  were set to zero and the unplated span ratio  $\rho$  was set to unity.

The predicted and measured deformations are shown in Table 1 for the Beams A – D. It is evident that the predicted tip deflections range from about 5.7% higher to about 0.8% lower than the measured deflections, whereas the predicted tip rotations are all higher than the measured rotations, ranging from a maximum of 8.7% to a minimum of about 3.2%. It is reasonable to suppose that the larger differences between predicted and measured results may be due to differences in the longitudinal elastic moduli of the Beams A – D which are not accounted for in the predicted values obtained from Eqs. 2 and 3.

Table 1

Comparison of unstiffened cantilever tip deformations with mid-span deflections and end rotations of unstiffened simply supported beams in three-point flexure [ $E = 21.11\text{kN/mm}^2$ ,  $G = 2.93\text{kN/mm}^2$ ,  $I = 3.303 \times 10^6\text{mm}^4$ ,  $A = 1.855 \times 10^3\text{mm}^2$ ,  $L = 2.5\text{m}$ ,  $\varphi_I = \varphi_A = 0$ ,  $\rho = 1$ ]

Beam	Test Number	Load (kN)	Deflection (mm)	Error (%)	Rotation (mrad)	Error (%)
A	-	4.418	21.13	5.65	24.75	8.74
	3	4.418	20.00		22.76	
B	-	4.287	20.51	2.55	24.02	8.39
	3	4.287	20.00		22.16	
C	-	4.262	20.39	1.95	23.88	6.32
	3	4.262	20.00		22.46	
D	-	4.148	19.84	-0.80	23.24	3.24
	3	4.148	20.00		22.51	

Notes: Upper figures in each row are the values predicted with Eqs. 2 and 3 and the lower figures in each row are the test results given in Table 2 of [8]. The test rotations are the average of the two values at the supports. Error (%) = [(predicted value/test value) – 1] x 100.

The second set of results comparisons were obtained from Beams A – D after their tension flanges had been stiffened with CFRP strip and re-tested in three-point flexure. The unstiffened span ratios  $\rho$  of these beams ranged from 0 to 0.75. Comparison results for an additional fully stiffened beam, Beam E, are included in Table 2 together with those for Beams A – D. For these beams the elastic stiffnesses  $E$  and  $G$ , the geometric properties  $I$ ,  $A$  and the span  $L$  are the same as before. However, for the CFRP stiffened regions of the span  $\varphi_I$  and  $\varphi_A$  were set to 0.412 and 0.371 respectively.

It is evident, from Table 2, that the tip deflections predicted with Eq. 2 under-predict the measured deflections in the majority of cases when the beams are partially stiffened. The deflections range from 0.2% higher to 4.1% lower. The range of variation is slightly lower for partially stiffened than for unstiffened cantilevers. The tip rotations are all over-estimated by Eq. 3. They range from about 5.7% to 0.8% higher than the measured values. Again, this range of variation is somewhat smaller than when the cantilevers are unstiffened.

The third set of deformation results comparisons, shown in Table 3, are for fully stiffened ( $\rho = 0$ ) beams, i.e. they were stiffened by bonding the CFRP strip to the tension flange. The elastic stiffness and section properties of the beams were the same as before. However, their spans  $L$  ranged from 2.5m to 2.95m. Beam E was also tested upside down, so that its compression flange was fully stiffened.

It is evident from Table 3, that, in all cases, the tip deflection is under-predicted by Eq. 2 whereas the tip rotation is over-estimated by Eq. 3. The under-predicted tip deflection ranges from about 0.4% low to about 3.9% low and the over-estimated tip rotation ranges from about 2% high to 4.6% high.

Table 2

Comparison of partially stiffened cantilever tip deformations with mid-span deflections and end rotations of partially stiffened simply supported beams in three-point flexure [ $E = 21.11\text{kN/mm}^2$ ,  $G = 2.93\text{kN/mm}^2$ ,  $I = 3.303 \times 10^6\text{mm}^4$ ,  $A = 1.855 \times 10^3\text{mm}^2$ ,  $L = 2.5\text{m}$ ,  $\varphi_I = 0.412$ ,  $\varphi_A = 0.371$ ]

Beam	Unstiffened length ratio ( $\rho$ )	Test Number	Load (kN)	Deflection (mm)	Error (%)	Rotation (mrad)	Error (%)
A	0.25	-	5.825	19.92	-0.40	23.71	5.61
		3	5.825	20.00		22.45	
B	0.50	-	5.605	20.04	0.20	24.53	5.73
		3	5.605	20.00		23.20	
C	0.75	-	4.808	19.18	-4.10	23.50	0.77
		3	4.808	20.00		23.32	
D	0.00	-	5.693	19.30	-3.50	22.59	4.63
		3	5.693	20.00		21.59	
E	0.00	-	5.722	19.40	-3.00	22.70	4.66
		3	5.722	20.00		21.69	

**Notes:** Upper figures in each row are the values predicted with Eqs. 2 and 3 and the lower figures in each row are the test results given in Table 4 of [8]. The test rotations are the average of the two values at the supports. Error (%) = [(predicted value/test value) - 1] x 100.

Table 3

Comparison of fully stiffened cantilever tip deformations with mid-span deflections and end rotations of fully stiffened simply supported beams in three-point flexure [ $E = 21.11\text{kN/mm}^2$ ,  $G = 2.93\text{kN/mm}^2$ ,  $I = 3.303 \times 10^6\text{mm}^4$ ,  $A = 1.855 \times 10^3\text{mm}^2$ ,  $L = 2.5\text{m} - 2.95\text{m}$ ,  $\varphi_I = 0.412$ ,  $\varphi_A = 0.371$ ,  $\rho = 0$ ]

Beam	Span (m)	Test Number	Load (kN)	Deflection (mm)	Error (%)	Rotation (mrad)	Error (%)
1	2.95	-	3.603	19.93	-0.35	19.91	4.13
		1	3.603	20.00		19.12	
2	2.89	-	3.781	19.68	-1.60	20.05	2.51
		1	3.781	20.00		19.56	
E	2.50	-	5.722	19.40	-3.00	22.70	4.60
		2	5.722	20.00		21.72	
E†	2.50	-	5.673	19.23	-3.85	22.51	1.99
		1	5.673	20.00		22.07	

**Notes:** Upper figures in each row are the values predicted with Eqs. 2 and 3 and the lower figures in each row are the test results given in Table 5 of [8]. The test rotations are the average of the two values at the supports. Error (%) = [(predicted value/test value) - 1] x 100. † Beam tested upside down, i.e. with the CFRP strips bonded to the compression flange.

The final set of results comparisons apply to beams fully CFRP stiffened along their tension flanges. They were tested at two spans and at two load levels. The cross-section



properties were marginally different from the previously tested beams, so that their  $\phi_I$  and  $\phi_A$  values were 0.405 and 0.361 respectively. The results comparisons are shown in Table 4. The tip deflection is under-predicted by Eq. 2 and the tip rotation is, in the majority of cases, over-predicted by Eq. 3. The under-prediction of the tip deflection ranges from about 2.4% to 3.4% and the predicted tip rotation ranges from about 0.5% low to 1.4% high.

Two further observations may be made about the results in Table 4. The first is that the under-prediction of the tip deflection appears to increase somewhat as the load increases. And the second is that, unlike in the three previous sets of results comparisons, the tip rotations appear to be more accurately predicted than the tip deflections.

Table 4

Comparison of fully stiffened cantilever tip deformations with mid-span deflections and end rotations of fully stiffened simply supported beams in three-point flexure [ $E = 21.11\text{kN/mm}^2$ ,  $G = 2.93\text{kN/mm}^2$ ,  $I = 3.3049 \times 10^6\text{mm}^4$ ,  $A = 1.8645 \times 10^3\text{mm}^2$ ,  $L = 2.95\text{m}$  &  $3.756\text{m}$ ,  $\phi_I = 0.405$ ,  $\phi_A = 0.361$ ,  $\rho = 0$ ]

Beam	Span (m)	Test Number	Load (kN)	Deflection (mm)	Error (%)	Rotation (mrad)	Error (%)
1	3.756	-	0.891	9.74	-2.60	7.69	0.65
		3	0.891	10.00		7.64	
1*	3.756	-	2.209	24.15	-3.40	19.07	-0.52
		3	2.209	25.00		19.17	
2	2.950	-	1.829	9.76	-2.40	9.74	1.35
		2	1.829	10.00		9.61	
2*	2.950	-	3.630	19.37	-3.15	19.33	0.94
		3	3.630	20.00		19.15	

**Notes:** Upper figures in each row are the values predicted with Eqs. 2 and 3 and the lower figures in each row are the test results given in Table 6 of [8]. The test rotations are the average of the two values at the supports. Beams 1, 1\*, 2 and 2\* are the simply supported beams in Table 6 of [8]. Error (%) = [(predicted value/test value) – 1] x 100.

## 5. CONCLUDING REMARKS

The Method of Transformed Sections [12] has been used in conjunction with the Method of Influence Coefficients [13] to derive equations for predicting the tip deflection and rotation of partially CFRP stiffened pultruded GRP cantilevers.

The analogy between the deformations of a simply supported beam in three-point flexure and a tip-loaded cantilever has been used to *side-step* the need to test cantilever beams in order to generate data to verify the cantilever tip-deformation equations. It is widely recognised that truly rigid supports are difficult to simulate in beam tests.

Published deformation data for three-point flexure tests on partially CFRP stiffened pultruded GRP beams with simply supported ends have been used to verify the newly derived deformation equations for tip-loaded cantilevers.

It has been shown that the largest error in the predicted tip deflection is about 6% and is usually significantly smaller. Likewise, it has been shown that the largest error in the predicted tip rotation is about 8.7% and is also often significantly smaller. These

maximum percentage errors in the predicted deformations are not particularly large from the standpoint of structural design. It is, therefore, concluded that Eqs. 2 and 3 may be used to assess the serviceability (deformation) limit state of tip-loaded cantilevers.

The fact that the new equations have been shown to be accurate for cantilevers, i.e. beams with one clamped support, suggests that the equations derived in [7] are also valid for clamped ends, even though this was not able to be verified with the test data because of the inability to reproduce rigid supports in the tests.

## REFERENCES

1. Anon. "First hybrid I-girder bridge". *FRP International*, 1997;5: 4.
2. Witcher D.A. *Proceedings of the Second International Conference on Composites in Infrastructure (ICCI 98)*, Tucson, USA, 1998;2:327-340.
3. Head P.R. *Proceedings of the First International Conference on Advanced Composite Materials in Bridges and Structures (ACMBS 1)*, Sherbrooke, Canada, 1992:15-30.
4. Turvey G.J. *Proceedings of the First International Conference on Innovative Materials and Technologies for Construction and Restoration (IMTCR 2004)*, Lecce, Italy, 2004;1:578-588.
5. Anon. "Design guidance for strengthening concrete structures using fibre composite materials". Technical Report 55, 2<sup>nd</sup> edition, The Concrete Society, 2004.
6. Cadei J.M.C., Stratford T.J., Hollaway L.C., Duckett W.G. "Strengthening of metallic structures using externally bonded fibre-reinforced polymers". CIRIA Report C595, Construction Industry Research and Information Association, 2004.
7. Turvey G.J. "Structural analysis of CFRP-plated pultruded GRP beams". *Proceedings of the Institution of Civil Engineers: Structures and Buildings*, 2006;159:65-75.
8. Turvey G.J. "Analysis of bending tests on CFRP-stiffened pultruded GRP beams". *Proceedings of the Institution of Civil Engineers: Structures and Buildings*, 2007;160:37-49.
9. Turvey G.J. "Lateral buckling tests on rectangular cross-section pultruded GRP cantilever beams". *Composites Part B: Engineering*, 1996;27B:35-42.
10. Brooks R.J. and Turvey G.J. "Lateral buckling of pultruded GRP I-section cantilevers". *Composite Structures*, 1995;32:203-215.
11. Turvey G.J. "Effect of load position on the lateral buckling of pultruded GRP cantilevers – correlations between experiment and theory". *Composite Structures*, 1996;35:33-47.
12. Case J. and Chilver A.H. "Strength of materials". Edward Arnold, 1959.
13. Morice P.B. "Linear structural analysis: an introduction to the influence coefficient method applied to statically indeterminate structures". Thames and Hudson, 1969.
14. Anon. "EXTREN fiberglass structural shapes: design manual". Strongwell, 1989.